PHILOSOPHICAL TRANSACTIONS OF THE ROYAL SOCIETY A MATHEMATICAL, PHYSICAL & ENGINEERING SCIENCES

Many-Body Effects in Layered Systems [and Discussion]

J. A. White, J. C. Inkson, J. W. Wilkins, M. L. Cohen and M. J. Kelly

Phil. Trans. R. Soc. Lond. A 1991 **334**, 491-500
doi: 10.1098/rsta.1991.0029

Many-body effects in layered systems

By J. A. White† and J. C. Inkson

University of Exeter, Department of Physics, Stocker Road, Exeter EX4 4QL, U.K.

An investigation of quasi-particle properties is presented in single- and double-quantum-well systems as a function of electron density. Significant changes from bulk parameters are found with strong dependencies on the electron density and interwell separation. Low-energy plasmon modes are found to dominate the quasi-particle lifetime giving scattering rates up to an order of magnitude higher than optic phonons in these systems.

1. Introduction

The electronic properties of single and multiple layer quasi-two-dimensional systems have been studied extensively both experimentally and theoretically in recent years driven by both the technological importance and applications of the new semiconductor growth systems and by the appearance of new physics (Ando *et al.* 1982). Reduced dimensionality, changes in coupling to phonon modes, the effects of interface scattering, strain have all been considered. The study of many-body effects in two-dimensional systems is particularly interesting because, apart from the usual structural parameter variations available, the two-dimensional electron density can be varied continuously over a wide range in a single device and so provides the opportunity to test the theory in much more detail than is possible in bulk materials.

Many-body effects have been studied in silicon inversion layers (Ando *et al.* 1982; Smith & Stiles 1972; Ting *et al.* 1975; Ohkawa 1976; Vinter 1976) but recently, GaAs or AlAs quantum well systems have become the centre of attention. In such systems, because of the low GaAs band mass, many-body effects are not expected to be as important as in silicon. There are still significant exchange-correlation contributions to the subband structure (Kawamoto *et al.* 1980; Ando 1987), however, while the absence of extraneous intervalley and impurity scattering and the direct nature of the band gap have important theoretical and experimental advantages.

The central quantity in the calculation of quasi-particle properties is the electron self-energy. This requires the calculation of the screened electron–electron interaction which in turn involves the calculation and inversion of the dielectric response function the poles of which are the plasmons. Physically the self-energy can be thought of as arising largely from the virtual emission and absorption of plasmons with the other (single-particle excitations) playing a minor role and so the study of interaction effects is linked closely to that of plasmon properties.

There have been many calculations of the plasmon spectrum in single and multiple layers (Stern 1967; Dahl & Sham 1977; Eguiluz & Maradudin 1978; Tselis & Quinn 1982) up to superlattice systems (Grecu 1973; Hawrylak *et al.* 1985; King-Smith & Inkson 1986), i.e. an infinite array of parallel two-dimensional electron gases of equal

† Present address: Department of Theoretical Physics, University of Lund, Sölvegatan 14A, S-22362 Lund, Sweden.

electron density. The conclusion for the single-quantum-well system with one occupied band is that there are as many plasmon bands as there are electronic subbands. The lowest plasmon band being due to intraband and the higher bands interband polarization. Multiple-well systems support acoustic plasmon modes through the interlayer interaction, the number of such modes increasing with the number of layers. These plasmon modes have been measured in light scattering experiments (Olego *et al.* 1982; Fasol *et al.* 1986) and the agreement between theory and experiment has been good.

The energies of the plasmons are typically of the order of both the intersubband energies and, for typical experimental parameters, optical phonon energies. This together with the reduced dimensionality suggests that the self-energy and hence the quasi-particle parameters can be expected to show much more structure than in the case of bulk semiconductors. Few such calculations have been carried out, however, Hawrylak and co-workers (Hawrylak 1987; Hawrylak *et al.* 1988) have calculated the correlation energy, effective mass and quasi-particle lifetime within the RPA for quasi-particles in a superlattice. Here we shall concentrate on the properties of a single quantum well and two parallel quantum wells so that low-dimensional effects can be emphasized. These systems also offer the easiest possibility of experimentally varying the electron density within the same device.

2. Model

We first take the case of a single well; we consider the lowest two subbands, $n = 0, 1$, of a single modulation doped semiconductor quantum well of width a within the effective mass approximation. For simplicity we assume that only the lowest subband is occupied with an areal electron density N. We also assume that the subband wavefunctions are those of an infinite square well. This is expected to be a good enough approximation for symmetric quantum wells in the GaAs or GaAlAs system when the barrier height is high compared with the energy gap between the subbands. Electrons exhibit free particle-like behaviour in the plane of the well, with 'bare' mass m for each subband. The screening of the Coulomb interaction by the intrinsic semiconductor is described by a dielectric constant κ.

The hamiltonian for the system then is that of particles in a simple two-dimensional square well potential interacting via a Coulomb interaction $e^2/\kappa r$. The spatial part of the wavefunction for the single-particle state with parallel momentum $\boldsymbol{k}$, in subband n is thus

$$\psi_{\boldsymbol{k}}^{n}(\boldsymbol{r}) = \phi_n(z)\,\mathrm{e}^{\mathrm{i}\boldsymbol{k}\cdot\boldsymbol{\rho}},$$

where $\boldsymbol{r} = (\boldsymbol{\rho}, z)$ and any $\boldsymbol{k}$ dependence of the $\phi_n(z)$ is neglected. Denoting the corresponding annihilation operator for spin σ as $c_{\boldsymbol{k}n\sigma}$, the hamiltonian may be written

$$H = \sum_{\boldsymbol{q}n\sigma} t_{qn}\, c^{+}_{\boldsymbol{q}n\sigma}\, c_{\boldsymbol{q}n\sigma} + \frac{1}{2} \sum_{\substack{\boldsymbol{q}\neq\boldsymbol{0} \\ \boldsymbol{k}\boldsymbol{k}'\sigma\sigma' \\ ll'nn'}} V_q^{ll'nn'}\, c^{+}_{\boldsymbol{k}+\boldsymbol{q}l\sigma}\, c^{+}_{\boldsymbol{k}'-\boldsymbol{q}n\sigma'} c_{\boldsymbol{k}'n'\sigma'}\, c_{\boldsymbol{k}l'\sigma},$$

where $t_{qn} = E_n + q^2/2m$ are the 'single-particle' nth subband energies, with minima at $E_0 = 0$ and $E_1 = E_{\mathrm{g}}$.

$$V_q^{ll'nn'} = \frac{2\pi}{\kappa q} \int\int \mathrm{d}x\,\mathrm{d}x'\, \phi_l(x)\,\phi_{l'}(x)\,\mathrm{e}^{-q|x-x'|}\phi_n(x')\,\phi_{n'}(x') \equiv v_q\, D_q^{ll'nn'}$$

are the Coulomb matrix elements between subband wavefunctions $ll'nn'$ for a momentum exchange of $\hbar q$, $v_q = 2\pi/\kappa q$ the two-dimensional Fourier transform of the Coulomb interaction and D is the weighting factor. All other symbols have their usual meaning. In the hamiltonian (2) we have included all electron–electron interactions beyond the Hartree approximation in the second term.

From the orthonormality of the subband wavefunctions it is easy to show that, D^{0000}, D^{1111}, $D^{0011} \to 1$ and $D^{0101} \propto qa$ as $qa \to 0$, while all of these four terms are proportional to $1/qa$ for $qa \to \infty$. By symmetry we also have $D^{0001} \equiv D^{1110} \equiv 0$.

The RPA dielectric function for the system is most easily dealt with by considering the Fourier transform in the plane and then expressing it as a matrix in the subband pairs appropriate to the Coulomb matrix elements in equation (3), thus:

$$\epsilon_{\alpha\beta}(q, \omega) = \delta_{\alpha\beta} - V_q^{\alpha\beta} P_\beta(q, \omega),$$

where the index α, β are the subband pairs (00), (01), (11). We shall denote such subband pairs with Greek letters throughout this paper.

The calculation for the intrasubband polarization P_{00} has been performed by Stern (1967) and for the intersubband term P_{01} we use the formulation of King-Smith and Inkson (1986). Since only the lowest subband is occupied, $P_{11} \equiv 0$. The spectrum of excitations is given by the inverse dielectric matrix

$$\operatorname{Im} \epsilon^{-1}_{\alpha\beta}(q, \omega) \neq 0,$$

i.e. intraband electron–hole pairs when $\operatorname{Im}(P_{00}(q, \omega)) \neq 0$, interband electron–hole pairs when $\operatorname{Im}(P_{01}(q, \omega)) \neq 0$ and plasmons when $\det \epsilon_{\alpha\beta}(q, \omega) = 0$.

The intraband plasmon corresponds to charge density oscillations in the plane of the quantum well and has the well-known $\omega \propto q^{\frac{1}{2}}$ behaviour at long wavelengths. The interband plasmon corresponds to charge density oscillations across the well and its energy tends to a constant value in the $q \to 0$ limit. The excitation spectrum is shown in figure 1 for GaAs parameters ($m = 0.07$, $\kappa = 13$) when well width $a = 100$Å†, $N = 3.3 \times 10^{11}$ cm^{-2}, and the subband gap has been chosen as 30 meV. Also note that, by symmetry, there is no Landau damping of the intraband plasmons lying within the interband electron–hole continuum.

In the case of a double well, the effects we are concerned with arise from the coupling of the low-energy intraband plasmons. The model is, therefore, simpler and includes only a single subband in each well. We consider a system of two parallel two-dimensional electron gases, labelled $i = 1, 2$, with areal electron densities n_1, n_2 and with interlayer separation d, i.e. electrons are confined to move in the planes $z_1 = 0$, $z_2 = d$ with no tunnelling between the layers. The in-plane effective 'bare' mass is m and the background dielectric constant is κ. This model is sufficient to describe fairly accurately the electronic response properties of a doped double-quantum-well structure when only the lowest subband in each well is occupied. It neglects the finite width of the wells and also neglects the effect of intersubband transitions. The effect of finite well width could be included through the usual form factors for the Coulomb interaction. This reduces the short-range part of the interaction, but should produce, qualitatively, the same results.

The dielectric function becomes a 2×2 matrix in real space

$$\epsilon_{ij}(q, \omega) = \delta_{ij} - V_{ij}(q) P_j(q, \omega), \quad i, j = \text{layer } 1, 2,$$

† $1\text{Å} = 10^{-10}$ m.

Figure 1

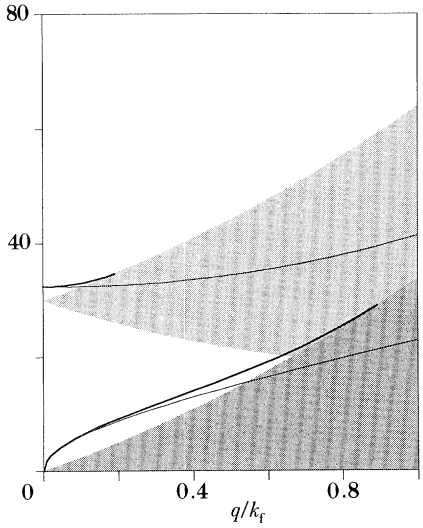

Figure 2

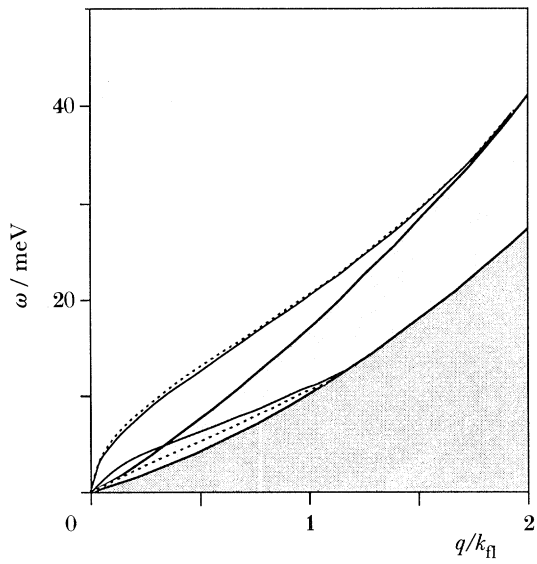

Figure 1. The plasmon modes (thick lines) of a doped quantum well with $n = 3.3 \times 10^{11}$ cm^{-2}, well width $a = 100$ Å, $E_g = 300$ meV, $\kappa = 13$, and $m = 0.07$. The shaded areas show the intraband and interband electron–hole continua. Also shown (thin lines) are the effective intraband and interband plasmon poles of equation (19), which approximate the plasmons for small q and lie inside the electron–hole pair bands for large q.

Figure 2. Plasmon spectrum for a two layer system with $n_1 = 10^{11}$ cm^{-2} ($k_{f1} = 8 \times 10^5$ cm^{-1}) and $n_2 = 4 \times 10^{11}$ cm^{-2} ($k_{f2} = 1.6 \times 10^6$ cm^{-1}) for $d = 100$ Å (solid lines) and for $d = 1000$ Å (broken lines). The shaded areas indicate the electron-hole continua of each layer. Plasmons in the shaded area are Landau damped as they may excite electron–hole pairs in the low density layer.

where q is the magnitude of the in-plane momentum, $P_i(q, \omega)$ is the polarization for layer i, and $V_{ij}(q)$ is the Coulomb interaction between layers i and j.

The screened interaction between layers i and j is then

$$W_{ij}(q, \omega) = \sum_l \epsilon^{-1}_{il}(q, \omega)\, V_{lj}(q)$$

and the poles of the screened interaction occur when

$$\det \epsilon_{ij}(q, \omega) = 0.$$

Unless the densities in the two layers are identical, no analytic solutions for the plasmon dispersion can, in general, be found. However, in the long wavelength limit, the high-frequency mode is obtained as just the $\omega_+ \propto q^{\frac{1}{2}}$ dependence of a plasmon in a single two-dimensional EG of density $(n_1 + n_2)$ and our numerical studies also show that the low-energy mode has the acoustic form $\omega_- \propto q$ at long wavelengths with the plasmon velocity decreasing as d decreases. Figure 2 shows the typical plasmon dispersion relations when $n_1 = 10^{11}$ cm^{-2}, $n_2 = 4 \times 10^{11}$ cm^{-2} for two separations, $d = 100$ Å and $d = 1000$ Å.

For the larger separation ω_- lies outside the electron–hole continua of both layers for small q and is therefore, like the ω_+ mode, undamped. For larger q values this mode lies inside the electron–hole pair band of layer 2 and is Landau damped, i.e. the

PHILOSOPHICAL TRANSACTIONS OF THE ROYAL SOCIETY A MATHEMATICAL, PHYSICAL & ENGINEERING SCIENCES

charge density oscillation may loose energy by exciting electron–hole pairs in layer 2. This damping is very weak, however.

3. Quasi-particle properties

For the single layer, by symmetry, the self-energy is diagonal in the subband index and each of the diagonal elements has two contributions which we label by the band index of the internal Green function

$$\Sigma_{nm}(k,E) = \frac{\mathrm{i}}{8\pi^3}\sum_l \int G^0_{ll}(\boldsymbol{k}+\boldsymbol{q}, E+\omega)\, W_{nllm}(q,\omega)\, \mathrm{e}^{\mathrm{i}\omega\delta}\, \mathrm{d}\boldsymbol{q}\, \mathrm{d}\omega$$

$$\equiv \sum_l \Sigma^l_{nn}(k,E)\, \delta_{nm},$$

where G^0_{nm} is the non-interacting Green function for electrons in subband n and the $W_{ll'nn'}$ are matrix elements of the screened interaction

$$W_{\alpha\beta}(q,\omega) = \sum_\gamma \epsilon^{-1}_{\alpha\gamma}(q,\omega)\, V^{\gamma\beta}_q.$$

Physically, Σ^n_{nn} corresponds to the virtual exchange of an intraband plasmon, the electron remaining within the subband whilst $\Sigma^{n'}_{nn}$ involves an interband plasmon and an intermediate state in the alternate subband.

The quasi-particle energies are then given approximately by

$$E_n(k) = t_{kn} + \Sigma_{nn}(k, t_{kn}).$$

For the double layer, the self-energy is calculated within the GW approximation on the mass shell. As there is no electron tunnelling between the layers, the self-energy is now diagonal in the layer index, i.e. it depends only on the effective intralayer interaction.

$$\Sigma_{mn}(k, E_0(k)) = \frac{\mathrm{i}\delta_{mn}}{8\pi^3}\int G_{mm}(\boldsymbol{k}+\boldsymbol{q}, E_0(k)+\omega)\, W_{mm}(q,\omega)\, \mathrm{d}\boldsymbol{q}\, \mathrm{d}\omega.$$

These relations are evaluated numerically to give the self-energy and hence the quasi-particle properties.

Figure 3 shows, for a single well, the real part of the self-energy at the quasi-particle peak, i.e. the contributions to the effective exchange correlation potentials as a function of parallel momentum.

First consider the two largest terms, Σ^0_{00} and Σ^1_{11}, which involve intraband (virtual) scattering processes. The self-energy in the lower subband has, generally, the larger magnitude. This means that, the effect of exchange and correlation is to increase the subband gap. The other significant feature of these two terms is the sharp downward 'spike' at around $k = 1.4k_\mathrm{f}$ which occurs at the threshold for an electron to emit plasmons. This is seen in three-dimensional systems as well (Lundqvist 1967; Overhauser 1971), but is more pronounced here because of the reduced dimensionality and incomplete screening. This 'spike' is largest in the higher subband because the electron–plasmon scattering is restricted in the lower subband by the Pauli principle.

The terms Σ^1_{00} and Σ^0_{11} involve intersubband scattering and are much smaller than the intraband scattering contributions because of the smaller Coulomb matrix

PHILOSOPHICAL TRANSACTIONS OF THE ROYAL SOCIETY A MATHEMATICAL, PHYSICAL & ENGINEERING SCIENCES

Figure 3

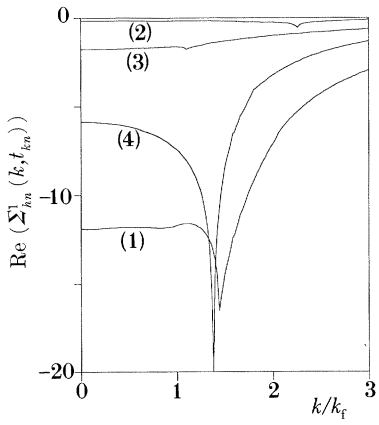

Figure 4

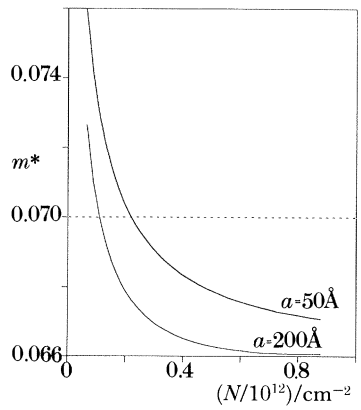

Figure 3. The real part of the contributions to the self-energy, evaluated at the quasi-particle peak, as a function of k. Σ^0_{00} (line (1)), Σ^1_{00} (line (2)), Σ^0_{11} (line (3)), and Σ^1_{11} (line (4)), as defined by equation (22), are shown. Here $N = 6.4 \times 10^{11}$ cm^{-2}, $E_g = 30$ meV and $a = 100$ Å.

Figure 4. Quasi-particle effective mass m^* as a function of electron density for well widths $a = 50$ Å and $a = 200$ Å.

elements. Again, each term has a spike corresponding to the threshold for emission of the effective intersubband plasmons. These are just visible at $k \approx 1.1k_f$ for Σ^0_{11} and $k \approx 2.3k_f$ for Σ^1_{00}.

3.1. *Effective masses*

The quasi-particle effective mass m^*, defined in terms of the quasi-particle group velocity v_g at the Fermi surface, is given by

$$\frac{1}{m^*} = \frac{1}{m} + \frac{1}{k_f}\frac{d}{dk}\operatorname{Re}\Sigma_{00}(k, t_{k0})\,|_{k=k_f}.$$

This can easily be calculated to the desired accuracy by numerical differentiation of the self-energy. We find that the behaviour of m^* is primarily determined by the intraband term in the self-energy Σ^0_{00}. Figure 4 shows m^* as a function of electron density N for two values of well width, $a = 50$ Å and $a = 200$ Å. Notice that m^* is significantly lower for the wider well. This is because the short-range part of the interaction is reduced in wide wells, which increases the importance of exchange effects (which tend to reduce m^*) while reducing the electron–plasmon coupling strength.

From figure 3 it is clear that there could be much more significant changes in the effective mass due to the very strong structure in the self-energy. However, for a single well, like a bulk material, the Fermi level lies well away from the region, corresponding to the plasmon emission threshold, in which the self-energy is varying rapidly. Lowering that threshold towards the Fermi energy could be expected to produce large changes in the effective mass. The most effective way of doing this is to introduce a second well. Coupling between the plasmons in the wells will introduce a lower energy 'acoustic' plasmon without changing the Fermi level. A suitable choice of densities and structural parameters also give the possibility of matching the plasmon velocity to the Fermi velocity so that resonant effects might occur.

Figure 5 shows the resulting variation in the Fermi level effective mass for a range of electron densities in the second well for a fixed separation. There is a wide range

PHILOSOPHICAL TRANSACTIONS OF THE ROYAL SOCIETY A MATHEMATICAL, PHYSICAL & ENGINEERING SCIENCES

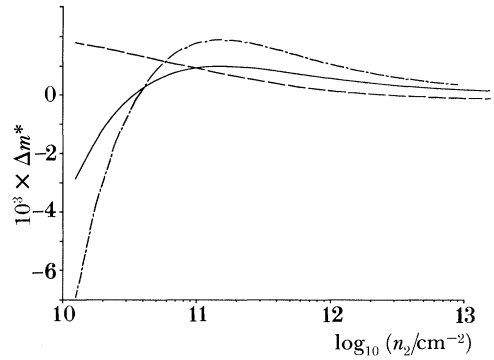

Figure 5. Difference Δm^* between effective mass at $d = 62.5$ Å and its value in a single two-dimensional EG ($d \to \infty$) as a function of density n_2 with $n_1 = n_2$ (solid curve) and $n_1 = 10^{11}$ cm^{-2} (broken curve). Also for the superlattice with $n = n_2$ (chain curve).

of behaviour with mass increases and decreases. This is to be expected since there are a number of effects in operation; the coupling to the higher plasmon mode, the acoustic plasmon velocity and the conservation of total oscillator strength. In particular the lower the energy of the acoustic plasmon with respect to the single-well energy, the lower its oscillator strength which reduces the overall effect. However, it is clear that this system would be a rich one for experimental investigation.

3.2. *Quasi-particle lifetime*

In a quantum well system the quasi-particle lifetime is governed by the possibility of the excitation of plasmons, phonons or electron–hole pairs. In our present calculations phonons are neglected and in the plasmon pole approximation used for most of these calculations, the electron–hole excitations have been subsumed within the plasmon oscillator strength. Calculations using the full RPA response function show the effect of the latter to be small anyway and what we are concerned with here is the magnitude of the lifetime, which is dominated by plasmon emission.

The inverse lifetime for quasi-particles of momentum k in subband n due to scattering into subband n' is

$$\tau^{-1}_{knn'} = -2 \operatorname{Im} \Sigma^{n'}_{nn}(k, t_{kn}). \tag{26}$$

Results for the inverse lifetimes due to intrasubband scattering as a function of quasi-particle momentum k, τ^{-1}_{k00} and τ^{-1}_{k11}, are shown in figure 6 for an electron density $N = 6.4 \times 10^{11}$ cm^{-2} and for well widths $a = 50$ Å and $a = 200$ Å. The inverse lifetime has been plotted in units of energy, with 6.56 meV corresponding to 10^{13} s^{-1}. Since the Coulomb matrix elements for intraband scattering are reduced as the well width increases, the larger well width corresponds to a lower emission threshold and also to a reduced scattering rate. The discontinuous change in the intraband scattering rate in the higher subband is typical of plasmons emission in a two-dimensional electron gas (Hawrylak *et al.* 1988). The discontinuity is not seen for intraband scattering within the lowest subband because of the restrictions of the exclusion principle on scattering.

Figure 7 shows the lifetime for intraband scattering for a double well for a range of separations. Both coupled plasmon modes contribute significantly for all separations. As the separation decreases, however, the range over which an acoustic dispersion holds increases. This is seen in the lifetime as both a large shift and a

Figure 6

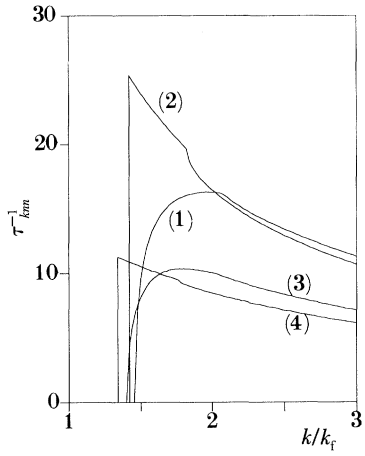

Figure 7

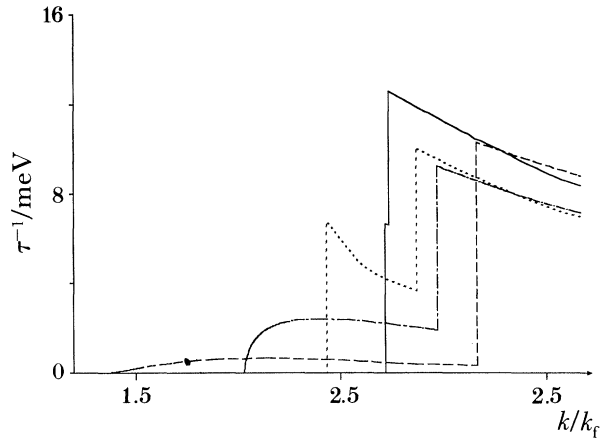

Figure 6. Inverse lifetime τ^{-1}_{knn} to intrasubband scattering within subband n as a function of quasiparticle parallel momentum k. Plotted for both subbands and for two well widths: $n = 0$, $a = 50$ Å (line (1)); $n = 1$, $a = 50$ Å (line (2)); $n = 0$, $a = 200$ Å (line (3)); $n = 1$, $a = 200$ Å (line (4)). Here $N = 6.4 \times 10^{11}$ cm^{-2} and $E_g = 30$ meV.

Figure 7. Inverse lifetime to plasmon emission in a two layer system, $n_1 = n_2 = 10^{11}$ cm^{-2}, for interlayer separations: 800 Å (solid), 300 Å (dotted), 200 Å (chain), 100 Å (broken).

functional change (to $(k - k_t)^{1.5}$) in the threshold, corresponding physically to the increasing preponderance of small-angle scattering allowed. (The equivalent superlattice threshold by contrast has an exponent of 2.)

For the electron densities considered here, the rate for intrasubband scattering via the Coulomb interaction is large compared with other scattering processes, such as scattering from LO phonons (Mason & Das Sarma, 1987). Furthermore intraband plasmon emission generally corresponds to large momentum transfers (*ca.* k_f) so that it is a very effective channel for momentum relaxation. It is therefore expected to be the dominant scattering process in hot electron transport for either single or coupled wells. The intersubband scattering rate, although much lower than the intrasubband rate (*ca* 10%), is still significant. For $a = 200$ Å, the intersubband lifetime of about 10^{-12} s is still similar to that for interband relaxation by LO phonon emission (Ridley 1989; Tatham *et al.* 1989), however. It might therefore be expected that electron–electron interactions will become the dominant intrasubband relaxation process in wide wells for which the subband gap is small enough to restrict LO phonon emission.

These Coulomb scattering rates, both intraband and interband, increase as electron density increases. We find that the intraband scattered rate scales approximately as between $N^{\frac{1}{2}}$ and N, while the interband scattering rate scales approximately as N.

4. Conclusions

We have shown that the modification of the plasmon modes in layered systems can alter basic quasi-particle properties. These properties are sensitive to both the structure and electron densities involved and are therefore a prime area for the study of electron–electron interactions, plasmon modes and their influence upon the quasi-particle properties.

PHILOSOPHICAL TRANSACTIONS OF THE ROYAL SOCIETY A MATHEMATICAL, PHYSICAL & ENGINEERING SCIENCES

References

Ando, T. 1987 Theory of semiconductor heterostructures. In *Third Brazilian school of semiconductor physics* (ed. C. E. T. Gonçalves da Silva, L. E. Oliveira & J. R. Leite), pp. 23–45. World Scientific.

Ando, T., Fowler, A. B. & Stern, F. 1982 Electron properties of two dimensional systems. *Rev. mod. Phys.* **54**, 437–677.

Dahl, D. A. & Sham, L. J. 1977 Electrodynamics of quasi two dimensional systems. *Phys. Rev.* B**16**, 651–659.

Eguiluz, A. & Maradudin, A. A. 1978 Electromagnetic modes of an inversion layer on a semiconductor surface. *Ann. Phys.* **113**, 29–78.

Fasol, G., Hughes, H. P. & Ploog, K. 1986 Raman scattering by coupled layer plasmons and in plane two-dimensional single particle excitations in multi quantum well structures. *Surf. Sci.* **170**, 497–513.

Grecu, D. 1973 Plasmons in layered systems. *Phys. Rev.* B**8**, 1958–1967.

Hawrylak, P. 1987 Effective mass and lifetime in a layered electron gas. *Phys. Rev. Lett.* **59**, 485–488.

Hawrylak, P., Eliasson, G. & Quinn, J. J. 1985 Electron self energy, effective mass and lifetime in a layered electron gas. *Phys. Rev.* B**37**, 10187–10203.

Hawrylak, P., Ji-Wei Wu & Quinn, J. J. 1985 Intersubband collective excitations at the surface of a semiconductor superlattice. *Phys Rev.* B**32**, 5169–5182.

Kawamoto, G., Kalia, R. & Quinn, J. J. 1980 Exchange and correlation insemiconductor surface inversion layers. *Surf. Sci.* **98**, 589–598.

King-Smith, R. D. & Inkson, J. C. 1986 Real space inversion of the dielectric response function of a superlattice. *Phys. Rev.* B**33**, 5489–5493.

Lundqvist, B. I. 1967 Single particle spectrum of an electron gas. *Phys. Kondens. Mater.* **6**, 193–218.

Mason, B. A. & Das Sarma, S. 1987 Theory of polar scattering in semiconductor quantum structures. *Phys. Rev.* B**35**, 3890–3898.

Ohkawa, F. J. 1976 Quasiparticle in surface quantised states in silicon. *Surf. Sci.* **58**, 326–332.

Olego, D., Pinczuk, A., Gossard, A. C. & Wiegmann, W. 1982 Plasmon dispersion in a layered electron gas. *Phys. Rev.* B**26**, 7867–7879.

Overhauser, A. W. 1971 Simplified theory of electron correlations in metals. *Phys. Rev.* B**3**, 1888–1898.

Ridley, B. K. 1989 Electron scattering by confined LO polar phonons in a quantum well. *Phys. Rev.* B**39**, 5282–5291.

Smith, J. L. & Stiles, P. J. 1972 Electron–electron interaction continuously variable in the range $2.1 > r_s > 0.9$. *Phys. Rev. Lett.* **29**, 102–104.

Stern, F. 1967 Polarisability of a two dimensional electron gas. *Phys. Rev. Lett.* **18**, 546–548.

Tatham, M. C., Ryan, J. F. & Foxon, C. T. 1989 Time resolved Raman measurements of intersubband relaxation in GaAs quantum wells. *Phys. Rev. Lett.* **63**, 1637–1641.

Ting, C. S., Lee, T. K. & Quinn, J. J. 1975 Effective mass and g factors of interacting electrons in the surface inversion layer of silicon. *Phys. Rev. Lett.* **34**, 870–874.

Tselis, A. & Quinn, J. J. 1982 Collective modes of semiconducting space charge layers. *Surf. Sci.* **113**, 362–381.

Vinter, B. 1976 Correlation energy and effective mass of electrons in an inversion layer. *Phys. Rev.* B**13**, 4447–4458.

Discussion

J. W. Wilkins (*Ohio State University, U.S.A.*) How would the large internal strains and resulting electric fields effect screening in superlattices?

J. Inkson. The electric fields resulting from strain or other sources (applied fields,

PHILOSOPHICAL TRANSACTIONS OF THE ROYAL SOCIETY A MATHEMATICAL, PHYSICAL & ENGINEERING SCIENCES

space charge, etc.) redistribute the electron density within the ground state. This can change the quantum well potential profiles and the single-particle wavefunctions dramatically even in extreme cases splitting the quantum well electron density into two separate two-dimensional electron gases. The results of our treatment are, however, dependent primarily upon gross features such as the electron density in the layers and the orthogonality of states in differing subbands.

M. L. Cohen (*University of California, Berkeley, U.S.A.*). What about phonon effects? Shouldn't there be phonon–plasmon coupling and other effects since the energy ranges are similar?

J. Inkson. Yes of course; one of the interesting aspects of this system is precisely the similarity of the energy ranges. Farol *et al.* (1986) may already have seen phonon effect in their data. Our results show the plasma coupling to be much stronger than phonon but we are already working on incorporating the phonon–plasmon coupling into the problem.

M. J. Kelly (*GEC and Cavendish Laboratory, U.K.*). What is the probability of phonon emission by a 300 meV hot electron passing at right angles through a two-dimensional electron gas?

Additional reference

Farol, G., King-Smith, R. D., Richards, D., Ekenberg, U., Mestres, N. & Ploog, K. 1986 *Phys. Rev.* B**39**, 12695–12703.

PHILOSOPHICAL TRANSACTIONS OF THE ROYAL SOCIETY A MATHEMATICAL, PHYSICAL & ENGINEERING SCIENCES

Figure 1

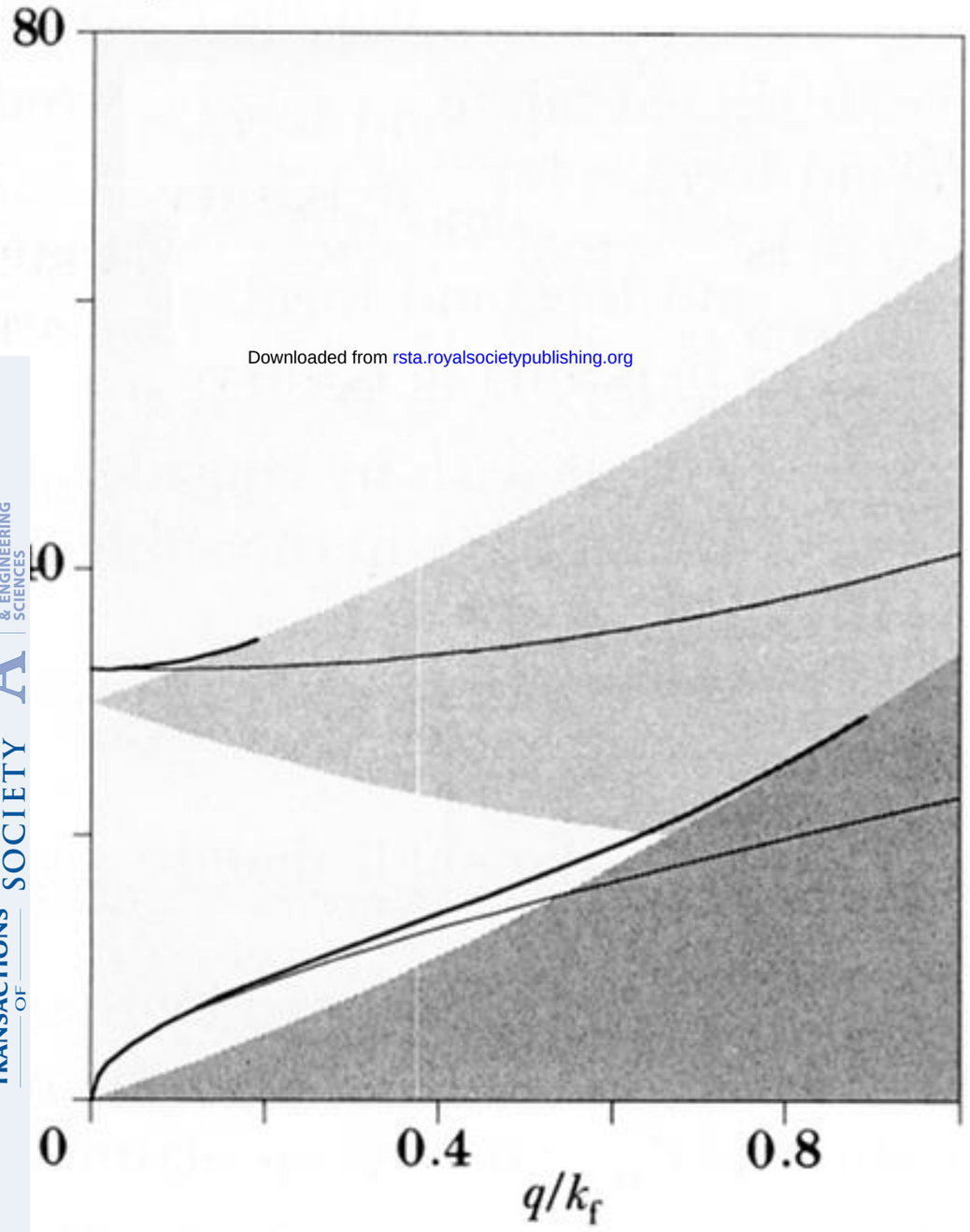

Figure 2

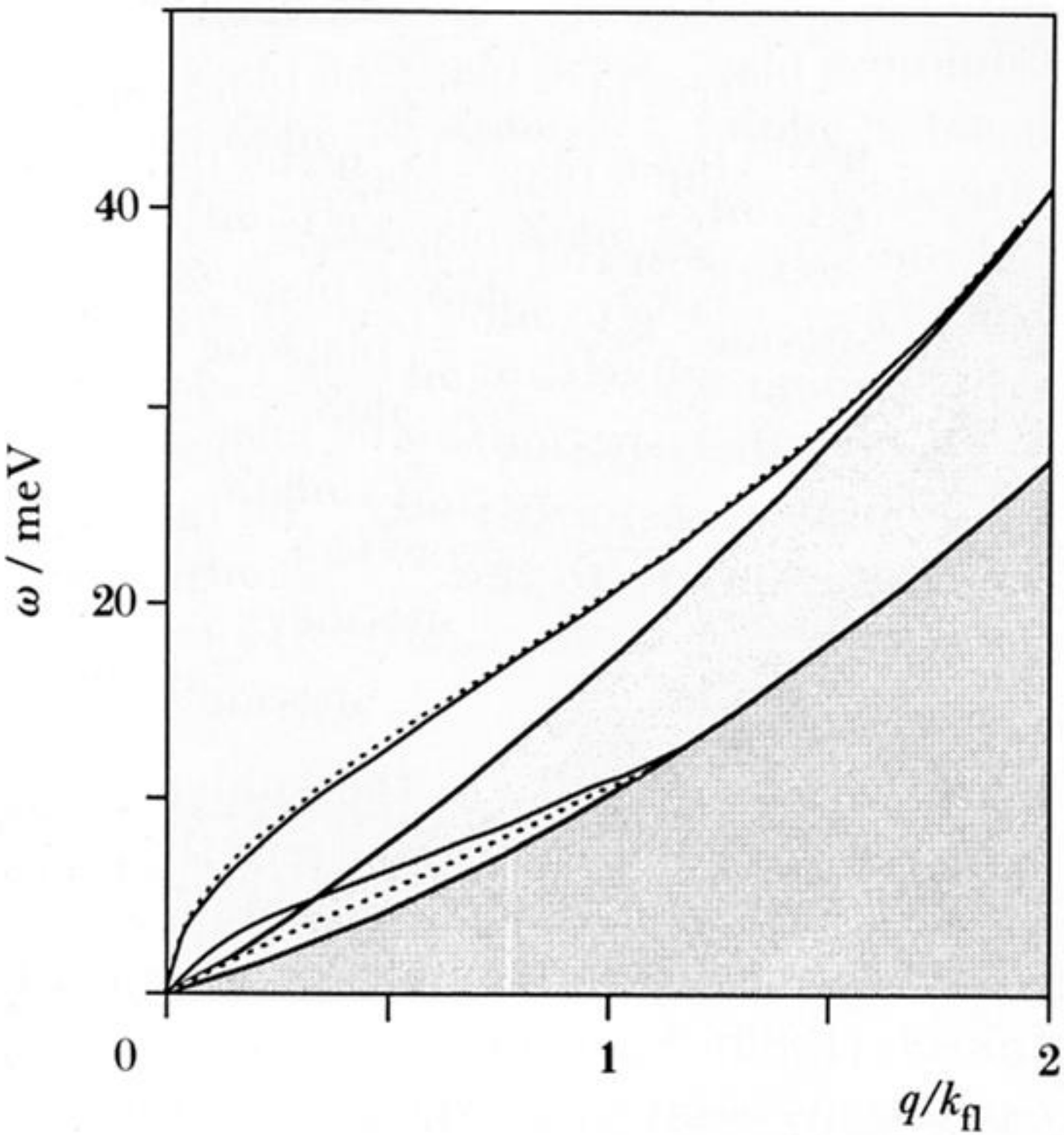

Figure 1. The plasmon modes (thick lines) of a doped quantum well with $n = 3.3 \times 10^{11}$ cm^{-2}, well width $a = 100$ Å, $E_g = 300$ meV, $\kappa = 13$, and $m = 0.07$. The shaded areas show the intraband and interband electron–hole continua. Also shown (thin lines) are the effective intraband and interband plasmon poles of equation (19), which approximate the plasmons for small q and lie inside the electron–hole pair bands for large q.

Figure 2. Plasmon spectrum for a two layer system with $n_1 = 10^{11}$ cm^{-2} ($k_{f1} = 8 \times 10^5$ cm^{-1}) and $n_2 = 4 \times 10^{11}$ cm^{-2} ($k_{f2} = 1.6 \times 10^6$ cm^{-1}) for $d = 100$ Å (solid lines) and for $d = 1000$ Å (broken lines). The shaded areas indicate the electron-hole continua of each layer. Plasmons in the shaded area are Landau damped as they may excite electron–hole pairs in the low density layer.